

## Hydrocarbon Synthesis via Photoenzymatic Decarboxylation of Carboxylic Acids

Zhang, Wuyuan; Ma, Ming; Huijbers, Mieke M.E.; Filonenko, Georgy A.; Pidko, Evgeny A.; van Schie, Morten; de Boer, Sabrina; Smith, Wilson A.; Hollmann, Frank; More Authors

**DOI**

[10.1021/jacs.8b12282](https://doi.org/10.1021/jacs.8b12282)

**Publication date**

2019

**Document Version**

Final published version

**Published in**

Journal of the American Chemical Society

**Citation (APA)**

Zhang, W., Ma, M., Huijbers, M. M. E., Filonenko, G. A., Pidko, E. A., van Schie, M., de Boer, S., Smith, W. A., Hollmann, F., & More Authors (2019). Hydrocarbon Synthesis via Photoenzymatic Decarboxylation of Carboxylic Acids. *Journal of the American Chemical Society*, 141(7), 3116-3120.  
<https://doi.org/10.1021/jacs.8b12282>

**Important note**

To cite this publication, please use the final published version (if applicable).  
Please check the document version above.

**Copyright**

Other than for strictly personal use, it is not permitted to download, forward or distribute the text or part of it, without the consent of the author(s) and/or copyright holder(s), unless the work is under an open content license such as Creative Commons.

**Takedown policy**

Please contact us and provide details if you believe this document breaches copyrights.  
We will remove access to the work immediately and investigate your claim.



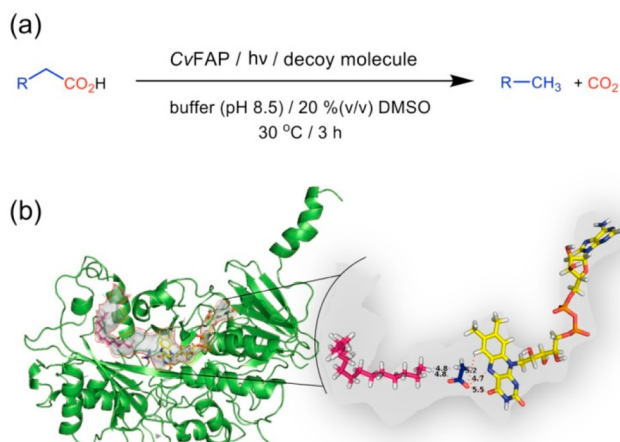


**Figure 1.** CvFAP-catalyzed photobiocatalytic decarboxylation reaction. (a) general reaction scheme and reaction conditions; (b) schematic representation of acetic acid coordinating to the catalytic flavin group together with tetradecane as decoy molecule filling up the substrate access channel. CvFAP (PDB: SNCC) is presented as a green cartoon showing the substrate channel as transparent gray surface, while FAD (yellow), acetic acid (blue) and tetradecane (magenta) are represented as sticks. The distances in angstroms from the carboxylate oxygen atom of acetic acid to FAD and from the C1-atom of tetradecane to both carbon atoms of acetic acid are indicated. First, acetic acid was docked into SNCC, then tetradecane was docked into the minimized result of the first docking using VINA in Yasara ([www.yasara.org](http://www.yasara.org)). The figure was prepared using PyMol (The PyMOL Molecular Graphics System, Version 2.0 Schrödinger, LLC).

might be applicable to enlarge the substrate scope of CvFAP (Figure 1b).

We propose using simple alkanes as decoy molecules, as cocatalysts, to accelerate the CvFAP-catalyzed decarboxylation of short-chain carboxylic acids.

## RESULTS AND DISCUSSION

We first evaluated CvFAP as a photobiocatalyst for the decarboxylation of acetic acid to methane in the presence of various decoy alkanes (Figure 2). For this the enzyme was overproduced in *Escherichia coli* BL21 (DE3). A typical time course of the reaction is shown in Figure 2a. No methane could be detected in the absence of CvFAP and only minor amounts were formed in the absence of active illumination (possibly due to the incomplete light-insulation of the reaction vessel). Moreover, no background activity was found in crude extracts prepared from *E. coli* cells containing an empty vector.  $^{13}\text{CH}_3\text{-CO}_2\text{H}$  was converted into  $^{13}\text{CH}_4$  (Figure S6). Most interestingly, the rate of methane accumulation was almost doubled in the presence of tridecane as decoy molecule, while also the robustness of the reaction increased significantly leading to more than a 3-fold increase of methane yield. The highest acceleration of methane production was achieved in the presence of tetradecane (Figure 2b). Both in the absence and presence of a decoy molecule, the enzyme reaction rate depended on the concentration of acetic acid (Figure 2c). In both cases half-maximal rates were obtained at comparable acetic acid concentrations (around 50 mM), suggesting that the decoy molecule did not facilitate the binding of the carboxylic acid but rather increased the enzyme reaction rate. When varying the concentration of the decoy molecule (Figure 2d), a saturation-type dependency of the reaction rate was observed. Furthermore, at elevated concentrations of the decoy

molecule an inhibitory effect was observed, which may be indicative for an ordered mode of binding of substrate and decoy molecule.

The rate of the photobiocatalytic decarboxylation reaction was linearly dependent on both the enzyme concentration (Figure S7) and the light intensity (Figure S8). The rate of the reaction in  $\text{D}_2\text{O}$  was approximately 1.5 times faster than the same reaction in  $\text{H}_2\text{O}$  (Figure S9). This inverse kinetic isotope effect most probably is due to an increased lifetime of the photoexcited flavin cofactor of CvFAP in  $\text{D}_2\text{O}$ , as well documented previously for other flavoproteins.<sup>31–33</sup> We interpret these findings with the lifetime of the photoexcited flavin of CvFAP being overall rate-limiting.

Encouraged by these promising results, we further evaluated the decarboxylation of a broader range of short-chain carboxylic acids (Table 1). The substrate scope of CvFAP was not limited to straight-chain carboxylic acids as also some branched and unsaturated carboxylic acids were converted at significant rates. Decarboxylation of acrylic acid and propionic acid was only possible with the assistance of decoy molecules. Notably, hydrogen gas was formed from the decarboxylation of formic acid. It also becomes clear from Table 1 (and Figures S11–19) that the most suited decoy molecule depends on the carboxylic acid used. In general the number of carbon atoms of substrate and decoy molecule should sum up to 16, which is in line with the previously reported optimal fatty acid chain length.<sup>28</sup> It is also interesting to note that the accelerating effect of the decoy molecule decreased with the chain length of the substrate carboxylic acids.

The quantum efficiency of the photobiocatalytic decarboxylation reactions was determined. Using acetic acid, butyric acid, pentanoic acid and hexanoic acid, the quantum efficiency (at photon flux  $13.8 \mu\text{E L}^{-1}\text{s}^{-1}$ ) was 0.008%, 1.3%, 3.2% and 2.7%, respectively (Figure S10). It should be noted that a direct comparison with the numbers reported in the initial report is difficult due to the lack of all necessary data.

A further insight into the decarboxylation mechanism was obtained in the framework of the density functional theory (DFT) and time-dependent (TD-DFT) density functional theory (PBE1PBE+D3(BJ)/6-311+G(d,p)+PCM(water)) analysis. These calculations were carried out on a representative model system mimicking the reactive complex of the flavin active site of the FDA and acetate anion as the representative substrate. Our calculations reveal the crucial role of the prearrangement of acetate in the vicinity of the N(5) site of the FAD ( $\text{CH}_3\text{COO}^- \cdots \text{FAD}$ , Figure S32). This van der Waals complex closely resembles the configuration found from the crystal structure analysis shown in Figure 1. Importantly, in the absence of the confinement caused by the protein residues of CvFAP, an alternative coordination mode dominated by H-bonding between the acetate anion and the N–H moiety of FAD is favored by ca. 20 kJ/mol. However, we were not able to identify a favorable decarboxylation path initiated from this structure, which is in agreement with the lack of decarboxylation activity of the free flavin (Figure S33).

When acetate substrate prearrangement is effective, the decarboxylation path starts from the  $\text{CH}_3\text{COO}^- \cdots \text{FAD}$  van der Waals complex exhibiting an absorption maximum at 467 nm.<sup>33</sup> Analysis of the respective frontier orbitals (HOMO, LUMO, Figure S32a) shows that photoexcitation of this molecular complex yields a  $\text{CH}_3\text{COO}^\bullet \cdots \text{FAD}^\bullet$  radical pair, from which the decarboxylation of the  $\text{CH}_3\text{COO}^\bullet$  proceeds rapidly via a highly favorable and low-barrier noncatalytic

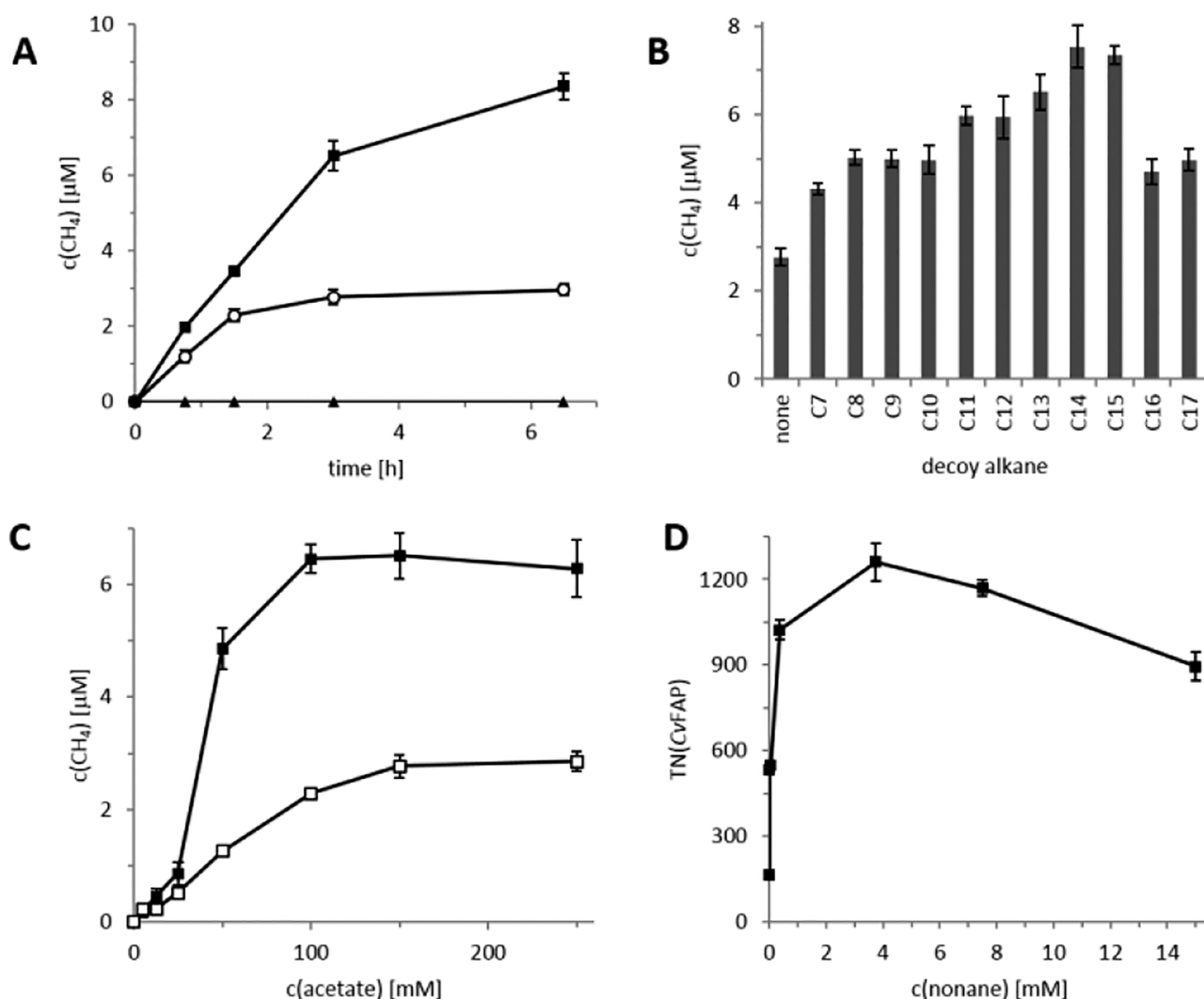


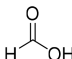
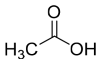
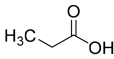
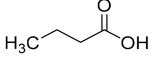
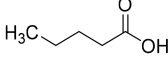
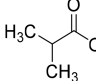
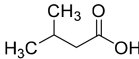
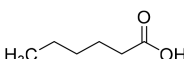
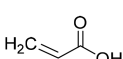
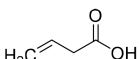
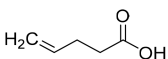
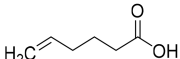
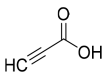
**Figure 2.** Photoenzymatic decarboxylation of acetic acid to methane (A–C). (A) Time course of methane formation performed with (■) and without decoy molecule tridecane (○), and in the absence of CvFAP (▲). Reaction conditions: [decoy molecule] = 15 mM, [CvFAP] = 6 μM, [acetic acid] = 150 mM, Tris–HCl buffer pH 8.5 (100 mM), 20% DMSO, 30 °C, blue light (450 nm). Methane concentration refers to product in the headspace of the reaction vial (4.0 mL of headspace plus 1.0 mL of liquid). (B) Effect of carbon length of decoy alkane on the methane formation. Reaction time: 3 h. (C) The rate-dependency of the methane production rate on the acetic acid concentration with (■) and without tridecane (□). Reaction time: 3 h. (D) Turnover number (TON) of CvFAP in the production of butane using nonane as decoy molecule. TON = mol<sub>butane</sub> × mol<sub>CvFAP</sub><sup>−1</sup>. The contribution of reaction without using nonane was subtracted. Condition: [CvFAP] = 6 μM, [pentanoic acid] = 150 mM, Tris–HCl buffer pH 8.5 (100 mM), 20% DMSO, 30 °C, 3 h. Error bars indicate the standard deviation of duplicate experiments (n = 2).

process. Computational studies propose that the generated CH<sub>3</sub> radical further binds the anionic flavin semiquinone resulting in the relaxation of the excited state to the original S<sub>0</sub> and the formation of a covalent dearomatized methylquinone flavin adduct. The overall decarboxylation reaction is slightly thermodynamically favorable ( $\Delta G^\circ = -5 \text{ kJ}\cdot\text{mol}^{-1}$ ) allowing thus for a smooth continuation of the catalytic cycle. The flavin adduct intermediate (CH<sub>3</sub>–FAD<sup>−</sup>) is then protonated to release the alkane product and regenerate the oxidized FAD closing the catalytic cycle (Figure S32b). Such a reaction pathway is also in agreement with the observed excellent selectivity of the photobiocatalytic decarboxylation reactions with all substrates used. This high selectivity makes the occurrence of free, C-centered radicals (at least for a prolonged period) highly unlikely.

## CONCLUSION

Overall, in the present study we have demonstrated the photobiocatalytic decarboxylation of short-chain carboxylic acids using the fatty acid photodecarboxylase from *Chlorella variabilis* NC64A (CvFAP). While the wild-type enzyme to some extent can convert also shorter substrates, the use of so-called decoy molecules significantly accelerates the reaction rate. Admittedly, the present reactions showed modest turnover numbers. However, we expect that engineering of both the enzyme and the decoy molecules will further increase the reaction rate and eventually render the CvFAP-catalyzed decarboxylation of a large scope of (waste) carboxylic acids into a viable approach for the generation of light hydrocarbons. Given the recent success in the photodecarboxylation of long fatty acids,<sup>28,34</sup> this work also demonstrates the broad potential of this photodecarboxylase for the application in biofuel synthesis and thus valorization of organic waste streams.

Table 1. Substrate Scope of the Photobiocatalytic Decarboxylation of Short-Chain Carboxylic Acids<sup>a</sup>

Entry	Substrate	Product	Best Decoy molecule	[Product] without decoy ( $\mu\text{M}$ )	[Product] with decoy ( $\mu\text{M}$ )	Acceleration (-fold)	TON (CvFAP) with decoy	Selectivity (%) <sup>[b]</sup>
1		H-H	C15	48.8 $\pm$ 5.6	291.7 $\pm$ 14.2	6.0	194	100
2		CH <sub>4</sub>	C14	2.7 $\pm$ 0.2	7.5 $\pm$ 0.5	2.5	5.0	100
3		H <sub>3</sub> C-CH <sub>3</sub>	C13	103 $\pm$ 7.9	347.1 $\pm$ 12.7	3.4	289	99.6 <sup>[c]</sup>
4		H <sub>3</sub> C-CH <sub>2</sub> -CH <sub>3</sub>	C12	382.2 $\pm$ 9.9	1090.5 $\pm$ 28.9	2.9	908.6	99.96 <sup>[c]</sup>
5		H <sub>3</sub> C-CH <sub>2</sub> -CH <sub>2</sub> -CH <sub>3</sub>	C9	860.7 $\pm$ 42.5	2440 $\pm$ 62.4	2.8	2034	99.99 <sup>[c]</sup>
6		H <sub>3</sub> C-CH <sub>3</sub>	C13	305.15 $\pm$ 36.1	1007 $\pm$ 57.3	3.3	839	99.8 <sup>[c]</sup>
7		H <sub>3</sub> C-CH <sub>3</sub> -CH <sub>3</sub>	C9	268.6 $\pm$ 19.4	940.2 $\pm$ 29	3.5	783.6	99.95 <sup>[c]</sup>
8 <sup>[d]</sup>		H <sub>3</sub> C-CH <sub>2</sub> -CH <sub>2</sub> -CH <sub>2</sub> -CH <sub>3</sub>	C14	1601.3 $\pm$ 40.1	1987.3 $\pm$ 28.7	1.2	1656	100
9		H <sub>2</sub> C=CH <sub>2</sub>	C13	0	2.1 $\pm$ 0.3	-	1.6	n.d.
10		H <sub>2</sub> C=CH-CH <sub>3</sub>	C12	1.08 $\pm$ 0.1	7.9 $\pm$ 0.7	7.3	6.9	100
11		H <sub>2</sub> C=CH-CH <sub>2</sub> -CH <sub>3</sub>	C10	24.27 $\pm$ 1.7	162 $\pm$ 11.3	6.8	134.5	100
12		H <sub>2</sub> C=CH-CH <sub>2</sub> -CH <sub>2</sub> -CH <sub>3</sub>	C9	188.3 $\pm$ 15.2	502.7 $\pm$ 10.9	2.7	418	100
13		HC $\equiv$ CH	C14	0	9.3 $\pm$ 1.2	-	7.1	100

<sup>a</sup>Reaction conditions: [decoy molecule] = 7.5 mM, [CvFAP] = 6  $\mu\text{M}$ , [substrate] = 150 mM, Tris-HCl pH 8.5 (100 mM), 20% DMSO, 30  $^{\circ}\text{C}$ , 3 h, blue light (450 nm), photon flux 13.8  $\mu\text{E}/\text{L}\cdot\text{s}$ . The standard deviation is based on duplicate experiments ( $n = 2$ ). The concentration refers to product in the headspace of the reaction vial (4.0 mL of headspace plus 1.0 mL of liquid). <sup>b</sup>Selectivity % = [target product]/([target product]+[other product])  $\times$  100, calculation based on GC. <sup>c</sup>0.4% propane, 0.038% ethane, 0.01% ethane, 0.2% isopentane and 0.05% propane were observed from Entries 3–7, accordingly. <sup>d</sup>Reaction was performed at 40  $^{\circ}\text{C}$ .

## ■ ASSOCIATED CONTENT

### Supporting Information

The Supporting Information is available free of charge on the ACS Publications website at DOI: 10.1021/jacs.8b12282.

Experimental details including the preparation of the cell free extracts, photoenzymatic reactions, length of decoy molecule on decarboxylation activity, GC chromatogram and DFC calculations (PDF)

## ■ AUTHOR INFORMATION

### Corresponding Author

\*f.hollmann@tudelft.nl

### ORCID

Ming Ma: 0000-0003-3561-5710

Evgeny A. Pidko: 0000-0001-9242-9901

Bastien O. Burek: 0000-0002-2180-7458

Willem J. H. van Berkel: 0000-0002-6551-2782

Frank Hollmann: 0000-0003-4821-756X

### Author Contributions

<sup>v</sup>W.Z., M.M. and M.M.E.H. contributed equally.

### Notes

The authors declare no competing financial interest.

## ■ ACKNOWLEDGMENTS

The Netherlands Organisation for Scientific Research is gratefully acknowledged for financial support through a VICI grant (no. 724.014.003). We thank Dr. Linda G. Otten and Dr. Fabio Tonin for support with the modelling.

## ■ REFERENCES

(1) Bozell, J. J.; Petersen, G. R. Technology development for the production of biobased products from biorefinery carbohydrates—the



US Department of Energy's "Top 10" revisited. *Green Chem.* **2010**, *12*, 539–554.

(2) Sheldon, R. A. Green and sustainable manufacture of chemicals from biomass: state of the art. *Green Chem.* **2014**, *16*, 950–963.

(3) Corma, A.; Iborra, S.; Velty, A. Chemical routes for the transformation of biomass into chemicals. *Chem. Rev.* **2007**, *107*, 2411–2502.

(4) Gallezot, P. Conversion of biomass to selected chemical products. *Chem. Soc. Rev.* **2012**, *41*, 1538–1558.

(5) Chu, S.; Majumdar, A. Opportunities and challenges for a sustainable energy future. *Nature* **2012**, *488*, 294–303.

(6) Potocnik, J. Renewable energy sources and the realities of setting an energy agenda. *Science* **2007**, *315*, 810–811.

(7) Obama, B. The irreversible momentum of clean energy. *Science* **2017**, *355*, 126–129.

(8) Aransiola, E. F.; Ojumu, T. V.; Oyekola, O. O.; Madzimbamuto, T. F.; Ikhu-Omoregbe, D. I. O. A review of current technology for biodiesel production: State of the art. *Biomass Bioenergy* **2014**, *61*, 276–297.

(9) Das, S.; Join, B.; Junge, K.; Beller, M. A general and selective copper-catalyzed reduction of secondary amides. *Chem. Commun.* **2012**, *48*, 2683–2685.

(10) Das, S.; Möller, K.; Junge, K.; Beller, M. Zinc-catalyzed chemoselective reduction of esters to alcohols. *Chem. - Eur. J.* **2011**, *17*, 7414–7417.

(11) Addis, D.; Das, S.; Junge, K.; Beller, M. Selective Reduction of Carboxylic Acid Derivatives by Catalytic Hydrosilylation. *Angew. Chem., Int. Ed.* **2011**, *50*, 6004–6011.

(12) Das, S.; Addis, D.; Zhou, S.; Junge, K.; Beller, M. Zinc-Catalyzed Reduction of Amides: Unprecedented Selectivity and Functional Group Tolerance. *J. Am. Chem. Soc.* **2010**, *132*, 1770–1771.

(13) Winkler, M. Carboxylic acid reductase enzymes (CARs). *Curr. Opin. Chem. Biol.* **2018**, *43*, 23–29.

(14) Finnigan, W.; Thomas, A.; Cromar, H.; Gough, B.; Snajdrova, R.; Adams, J. P.; Littlechild, J. A.; Harmer, N. J. Characterization of Carboxylic Acid Reductases as Enzymes in the Toolbox for Synthetic Chemistry. *ChemCatChem* **2017**, *9*, 1005–1017.

(15) Akhtar, M. K.; Turner, N. J.; Jones, P. R. Carboxylic acid reductase is a versatile enzyme for the conversion of fatty acids into fuels and chemical commodities. *Proc. Natl. Acad. Sci. U. S. A.* **2013**, *110*, 87–92.

(16) Venkatasubramanian, P.; Daniels, L.; Rosazza, J. P. N. Reduction of Carboxylic Acids by *Nocardia* Aldehyde Oxidoreductase Requires a Phosphopantetheinylated Enzyme. *J. Biol. Chem.* **2007**, *282*, 478–485.

(17) Ni, Y.; Hagedoorn, P. L.; Xu, J. H.; Arends, I.; Hollmann, F. A biocatalytic hydrogenation of carboxylic acids. *Chem. Commun.* **2012**, *48*, 12056–12058.

(18) Lu, C.; Shen, F.; Wang, S.; Wang, Y.; Liu, J.; Bai, W.-J.; Wang, X. An Engineered Self-Sufficient Biocatalyst Enables Scalable Production of Linear  $\alpha$ -Olefins from Carboxylic Acids. *ACS Catal.* **2018**, *8*, 5794–5798.

(19) Dennig, A.; Kurakin, S.; Kuhn, M.; Dordic, A.; Hall, M.; Faber, K. Enzymatic Oxidative Tandem Decarboxylation of Dioic Acids to Terminal Dienes. *Eur. J. Org. Chem.* **2016**, *2016*, 3473–3477.

(20) Zachos, L.; Gassmeyer, S. K.; Bauer, D.; Sieber, V.; Hollmann, F.; Kourist, R. Photobiocatalytic decarboxylation for olefin synthesis. *Chem. Commun.* **2015**, *51*, 1918–1921.

(21) Dennig, A.; Kuhn, M.; Tassoti, S.; Thiessenhusen, A.; Gilch, S.; Bültner, T.; Haas, T.; Hall, M.; Faber, K. Oxidative Decarboxylation of Short-Chain Fatty Acids to 1-Alkenes. *Angew. Chem., Int. Ed.* **2015**, *54*, 8819–8822.

(22) Hamid, S.; Ivanova, I.; Jeon, T. H.; Dillert, R.; Choi, W.; Bahnemann, D. W. Photocatalytic conversion of acetate into molecular hydrogen and hydrocarbons over Pt/TiO<sub>2</sub>: pH dependent formation of Kolbe and Hofer-Moest products. *J. Catal.* **2017**, *349*, 128–135.

(23) Esteves, L. M.; Brijaldo, M. H.; Passos, F. B. Decomposition of acetic acid for hydrogen production over Pd/Al<sub>2</sub>O<sub>3</sub> and Pd/TiO<sub>2</sub>: Influence of metal precursor. *J. Mol. Catal. A: Chem.* **2016**, *422*, 275–288.

(24) Rebelein, J. G.; Lee, C. C.; Hu, Y.; Ribbe, M. W. The in vivo hydrocarbon formation by vanadium nitrogenase follows a secondary metabolic pathway. *Nat. Commun.* **2016**, *7*, 13641.

(25) Beller, H. R.; Rodrigues, A. V.; Zargar, K.; Wu, Y.-W.; Saini, A. K.; Saville, R. M.; Pereira, J. H.; Adams, P. D.; Tringe, S. G.; Petzold, C. J.; Keasling, J. D. Discovery of enzymes for toluene synthesis from anoxic microbial communities. *Nat. Chem. Biol.* **2018**, *14*, 451–457.

(26) Peralta-Yahya, P. P.; Zhang, F.; del Cardayre, S. B.; Keasling, J. D. Microbial engineering for the production of advanced biofuels. *Nature* **2012**, *488*, 320.

(27) Bornscheuer, U. T.; Huisman, G. W.; Kazlauskas, R. J.; Lutz, S.; Moore, J. C.; Robins, K. Engineering the third wave of biocatalysis. *Nature* **2012**, *485*, 185–194.

(28) Sorigué, D.; Légeret, B.; Cuiné, S.; Blangy, S.; Moulin, S.; Billon, E.; Richaud, P.; Brugière, S.; Couté, Y.; Nurizzo, D.; Müller, P.; Brettel, K.; Pignol, D.; Arnoux, P.; Li-Beisson, Y.; Peltier, G.; Beisson, F. An algal photoenzyme converts fatty acids to hydrocarbons. *Science* **2017**, *357*, 903–907.

(29) Zilly, F. E.; Acevedo, J. P.; Augustyniak, W.; Deege, A.; Häusig, U. W.; Reetz, M. T. Tuning a P450 Enzyme for Methane Oxidation. *Angew. Chem., Int. Ed.* **2011**, *50*, 2720–2724.

(30) Kawakami, N.; Shoji, O.; Watanabe, Y. Use of Perfluorocarboxylic Acids To Trick Cytochrome P450BM3 into Initiating the Hydroxylation of Gaseous Alkanes. *Angew. Chem., Int. Ed.* **2011**, *50*, 5315–5318.

(31) Staudt, H.; Oesterhelt, D.; Grininger, M.; Wachtveitl, J. Ultrafast Excited-state Deactivation of Flavins Bound to Dodecin. *J. Biol. Chem.* **2012**, *287*, 17637–17644.

(32) McGuire, R.; Feldman, I. The quenching of tyrosine and tryptophan fluorescence by H<sub>2</sub>O and D<sub>2</sub>O. *Photochem. Photobiol.* **1973**, *18*, 119–124.

(33) Bonetti, C.; Mathes, T.; van Stokkum, I. H. M.; Mullen, K. M.; Groot, M.-L.; van Grondelle, R.; Hegemann, P.; Kennis, J. T. M. Hydrogen bond switching among flavin and amino acid side chains in the BLUF photoreceptor observed by ultrafast infrared spectroscopy. *Biophys. J.* **2008**, *95*, 4790–4802.

(34) Huijbers, M. M. E.; Zhang, W.; Tonin, F.; Hollmann, F. Light-Driven Enzymatic Decarboxylation of Fatty Acids. *Angew. Chem., Int. Ed.* **2018**, *57*, 13648–13651.